EJECTA SIZE RESULTING FROM HYPERVELOCITY IMPACTS OF ALUMINUM ALLOY SPHERES ON ALUMINUM ALLOY TARGETS

Masahiro Nishida[(1)], Kenta Nozaki[(2)], Koichi Hayashi[(2)], Sunao Hasegawa[(3)]

[(1)] Nagoya Institute of Technology, Gokiso-cho, Showa-ku, Nagoya 466-8555, Japan, Email: nishida.masahiro@nitech.ac.jp
[(2)] Nagoya Institute of Technology, Gokiso-cho, Showa-ku, Nagoya 466-8555, Japan
[(3)] Institute of Space and Astronautical Science, Japan Aerospace Exploration Agency, 3-3-1, Yunodai,Chuo, Sagamihara, Kanagawa, 229- 8510 Japan

ABSTRACT

The effects of projectile impact velocity on ejecta fragment size were investigated by striking aluminum alloy 6061-T6 targets with 3.2-mm-diameter aluminum alloy 2017-T4 spheres at velocities ranging from 2 to 6 km/s. The two-stage light-gas gun at the Institute of Space and Astronautical Science (ISAS)/ Japan Aerospace Exploration Agency (JAXA), was used for the experiments. To examine the scattering angles of ejecta, a witness plate (150 mm × 150 mm, 2 mm in thickness) made of copper C1100P-1/4H, with a 30-mm hole in the center, was placed 50 mm in front of the target. The behavior of ejected fragments was observed using a high-speed video camera. The projected areas of ejecta collected from the test chamber after the impact experiments were measured.

1 INTRODUCTION

Space debris has no useful purpose and often strikes spacecraft and space stations at velocities over several kilometers per second. The International Space Station (ISS) employs shields, such as the Whipple bumper and stuffed Whipple bumper, to protect itself from space debris. When space debris perforates the Whipple shields and stuffed Whipple bumper, debris clouds are formed. In comparison, projectiles with low kinetic energy—those with small size or low velocity—do not perforate the bumpers and outer surfaces of spacecraft and space stations; instead, they form craters on these surfaces. In such cases, fragments from the target surface are ejected and fragments of the projectile are scattered widely. These fragments (known as secondary debris) become new debris, as pointed out by Murr and his coworkers [1]. They studied hypervelocity impacts of projectiles on thick targets and examined the impact fragmentation of projectiles experimentally and numerically [2]. The international standard for test procedures to evaluate spacecraft material ejecta was published in 2012 [3]. Many studies have been conducted on related phenomena [4, 5]. However, the size distribution of such generated fragments and ejected fragments has not yet been fully elucidated [6], whereas numerous studies have analyzed the impacts of projectiles on thin plates.

In this study, the size distribution of the projected area of ejecta fragments collected from the test chamber were examined in detail and the witness plates were observed after the experiments. The ejection behavior of fragments was observed using a high-speed video camera. The effects of projectile impact velocity on ejecta were investigated. An experimental formula for the cumulative number distribution of the projected areas of ejecta is proposed.

2 EXPERIMENTAL SETUP

Aluminum alloy 2017-T4 spheres with a diameter of 3.2 mm (1/8 inches) and aluminum alloy 6061-T6 targets with a thickness of 30 mm and a diameter of 95 mm were employed. The two-stage light-gas gun at the Institute of Space and Astronautical Science (ISAS)/Japan Aerospace Exploration Agency (JAXA), was used at velocities ranging from 2 to 6 km/s. The effects of impact velocity on the ejecta fragment size were investigated. A witness plate (150 mm × 150 mm, 2 mm in thickness) made of copper C1100P-1/4H, with a 30-mm hole in the center, was placed 50 mm in front of each target, as shown in Fig. 1. The ejection behavior of the fragments was observed using a high-speed video camera (HPV-1, Shimadzu Corporation). The ejecta were collected from the test chamber after impact to measure the ejecta size.

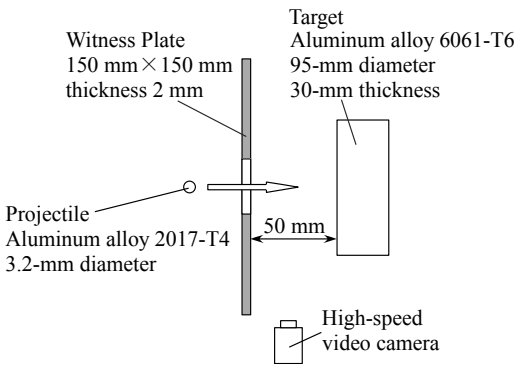

Figure 1. Experimental setup for normal impact

Proc. '6th European Conference on Space Debris'
Darmstadt, Germany, 22–25 April 2013 (ESA SP-723, August 2013)

Table 1 Mechanical properties of projectile and target

	Vickers hardness	Density [Mg/m^3]	Mass [g] (3.2 mm in diameter)
Aluminum alloy 2017-T4	118	2.7	0.05
Aluminum alloy 6061-T6	110	2.7	—

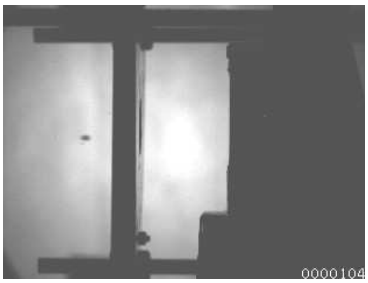

(a) 24 μs before impact

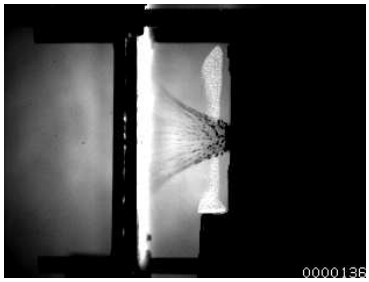

(b) 8 μs after impact

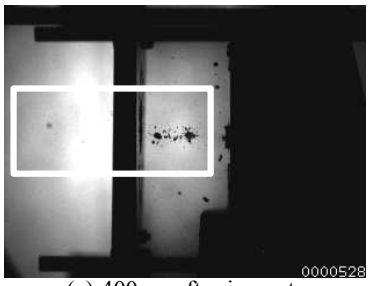

(c) 400 μs after impact

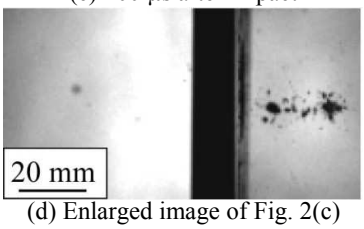

(d) Enlarged image of Fig. 2(c)

Figure 2. High-speed video images of normal impact of projectiles at an impact velocity of 4.05 km/s

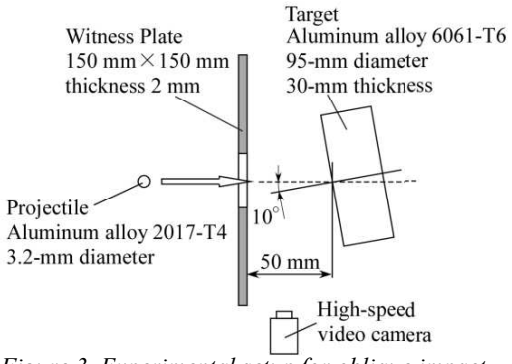

Figure 3. Experimental setup for oblique impact

3 RESULTS AND DISCUSSION

3.1 Normal impact

Figs. 2(a)–(d) show high-speed video images of a projectile striking a target perpendicularly at an impact velocity of 4.05 km/s. Fig. 2(b) shows that just after impact, an ejecta cone was formed. The velocity of the ejecta cone (the velocity of the ejecta cone tip) was calculated to be 3.75 km/s by measuring the movement of the ejecta cone tip in the images. Three large ejecta were observed passing through the hole of the witness plate in Fig. 2(c). It was estimated from the projectile size before impact in Fig. 2(a) and the ejecta size in Fig. 2(d), which is an enlarged image of Fig. 2(c), that the sizes of the large ejecta were approximately 4.5 mm, 3.5 mm, and 5 mm in length. However, no such large ejecta were collected from the test chamber after the impact experiments. We assumed that these large ejecta entered the launch tube or a small interspace around the launch tube. To collect such large ejecta, targets were then inclined from the axis of the launch tube, as shown in Fig. 3. When projectiles strike targets at an incidence angle close to normal, e.g., less than 25°, the crater shape is the same as that of normal impacts [7, 8]. Therefore, we predicted that with an impact angle of 10°, the large ejecta could be collected, and the ejecta shape and behavior would be almost the same as that for normal impact.

3.2 Oblique impact

Figs. 4(a)–(c) show high-speed video images of a projectile striking a target obliquely at an impact velocity of 4.28 km/s. Fig. 4(b) shows that the large ejecta shown in Fig. 4(a) did not pass through the hole of the witness plate. It was estimated from Fig. 4(c), which is an enlarged image of Fig. 4(b), that the size of the large ejecta was approximately 4 mm in length. Such large ejecta was collected from the test chamber after the impact experiments. Inclining the targets was effective for collecting large ejecta coming from

projectiles.

Fig. 5 shows the images of the witness plates after the experiments. We observed a ring on each plate consisting of many silver-colored indentations. In addition, outside each ring, we observed small radial and larger indentations (in many cases, silver-colored). In the case of normal impact in Fig. 5(a), the center of the indentation ring was within the hole of the witness plate. In such a case, it is easily predicted that ejecta rebounding off the target would pass through the hole of the witness plate. However, in the case of oblique impact in Fig. 5(b), the center of the elliptical indentation ring was outside the hole. On the basis of geometric relationships, the oblique angle was decided to be 10° so that rebound projectiles would not pass through the hole of the witness plate. A predictable result was ensured. However, no small indentations near the center of the ring resulting from the impact of large ejecta were observed on the witness plate near the hole. It was predicted from the images that the impact velocity of the ejecta on the witness plate was approximately 100 m/s. A velocity of 100 m/s is not hypervelocity, but it is not very slow. The main reason why indentations resulting from the impact of large ejecta were not observed is unclear. Further experiments and observations are required.

(a) 800 μs after impact

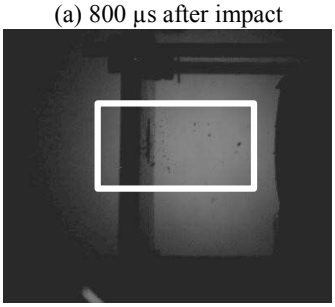

(b) 1188 μs after impact

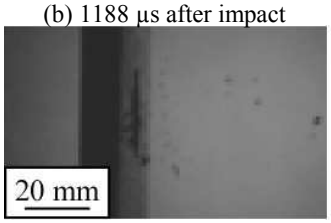

(c) Enlarged image of Fig. 4(b)

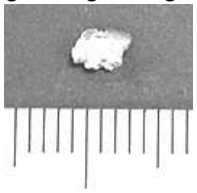

(d) Large ejecta collected from the test chamber

Figure 4. High-speed video images of oblique impact (impact angle 10°) of projectiles at 4.28 km/s.

3.3 Comparison of ejecta size distributions

Fig. 6 shows the cumulative number distribution of the projected areas of ejecta collected from the test chamber. The projected area A_e and size (length a, width b, thickness c) of the ejecta were defined as in Fig. 7. The photographs of ejecta were taken by a camera, and the images were analyzed using an image analysis software (image J) to obtain the projected areas of ejecta. Only ejecta having length greater than 0.5 mm were measured. In the case of oblique impact, large ejecta were collected (see Fig. 8) and the cumulative number of ejecta was greater. It was found that oblique impact was a better way to collect ejecta fragments. The following hypothesis about the cumulative number distribution of ejecta, as shown in Fig. 9, was considered. When the impact velocity was 2 km/s, there was a single large ejecta, namely the deformed projectile. As impact velocity increased, projectile fragmentation increased and ejecta smaller than original projectile size was collected. When the impact velocity increased to 6 km/s, large ejecta coming from the target was formed.

(a) Normal impact, 4.05 km/s

(b) Oblique impact, 4.28 km/s

Figure 5. Indentation observations on witness plates

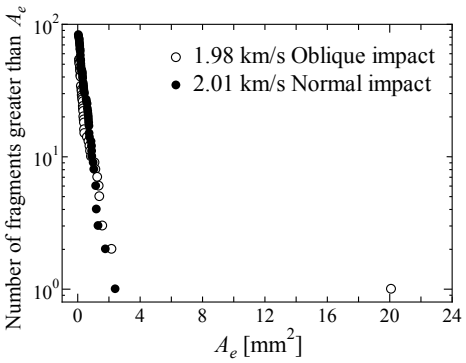

(a) Impact velocity, 2 km/s

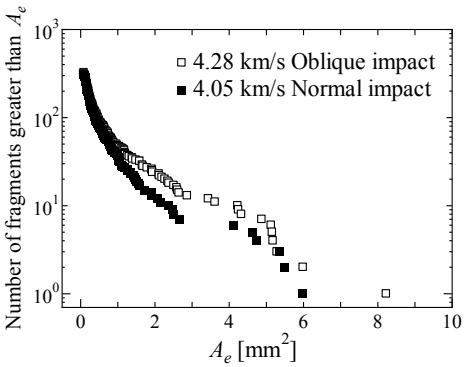

(b) Impact velocity, 4 km/s

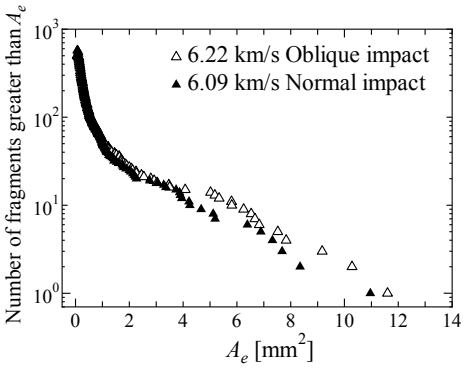

(c) Impact velocity, 6 km/s

Figure 6. Cumulative number distribution of projected area of ejecta

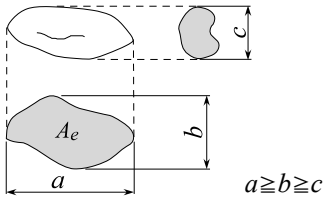

Figure 7. Definition of ejecta size

Figure 8. Large ejecta collected from the test chamber, subjected to oblique impact at 2.01 km/s

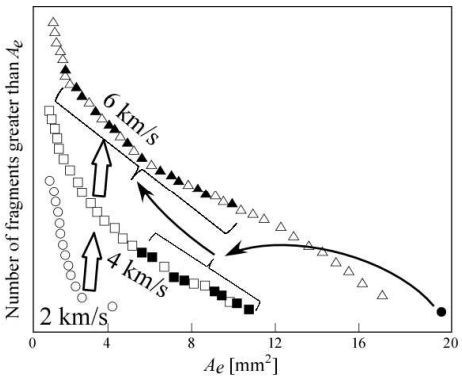

Figure 9. Hypothesis about cumulative number distribution of ejecta size

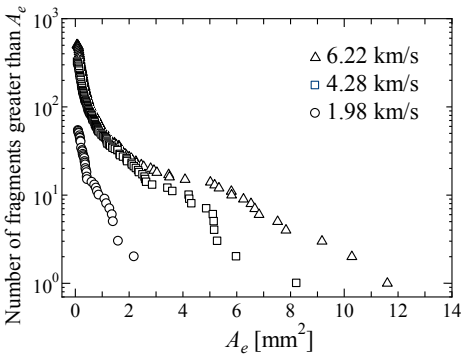

(a) Effects of impact velocity

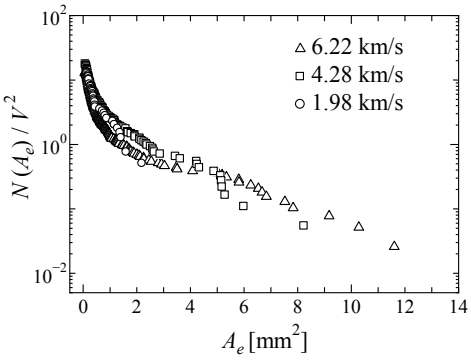

(b) Vertical axis divided by the square of impact velocity

Figure 10. Cumulative number distribution of projected area of ejecta size

3.4 Effects of impact velocity on ejecta size distribution

The effects of impact velocity on the cumulative number distribution were examined in Fig. 10(a). The projected area of ejecta on the horizontal axis and the cumulative number of ejecta on the vertical axis increased with increasing impact velocity. We studied dividing the vertical axis and/or horizontal axis by the projectile impact velocity or by the square of the projectile impact velocity. When the vertical axis was divided by the square of the projectile impact velocity, the results of all three impact velocities lay on a single curve, as shown in Fig. 11.It appears that the square of the projectile impact velocity is important to the cumulative number distribution of the projected area of ejecta. This result is different from our previous results on hypervelocity impact of polycarbonate projectiles on aluminum alloy targets, in which the vertical axis divided by the projectile impact energy was important [9]. The reason for this is unclear and further experiments are required.

3.5 Bilinear distribution of ejecta size

A bilinear exponential distribution approach was considered to model the cumulative number distribution of the projected areas. The following equation for bilinear exponential distribution [10] was used.

$$\frac{N(A_e)}{V^2} = a_1 \exp[b_1 A_e] + a_2 \exp[b_2 A_e] \qquad (1)$$

By fitting Eq. 1 to the three experimental results, the coefficients a_1, a_2, b_1, and b_2 were determined using the least squares technique.

$$\frac{N(A_e)}{V^2} = 18.48 \exp[-5.07 A_e] + 2.85 \exp[-0.51 A_e] \qquad (2)$$

Eq. 2 is in reasonable agreement with the experimental results for 2 km/s, 4 km/s, and 6 km/s, as shown in Fig. 12. To examine the degree of coincidence (goodness of fit), the coefficient of determination (R^2) was calculated. In the cases of the impact velocities of 4.28 km/s and 6.22 km/s, R^2 was over 0.99 and 0.97, respectively. In the case of 1.98 km/s, R^2 was only 0.64. However, when the large ejecta of the deformed projectile (A_e = 20.1 mm^2) was excluded, R^2 improved to 0.95.

4 CONCLUSIONS

The projected areas of ejecta collected from the test chamber were examined in detail. The oblique impact of projectiles was useful for collecting more ejecta. The cumulative number of the projected areas of ejecta was proportional to the square of the projectile impact velocity

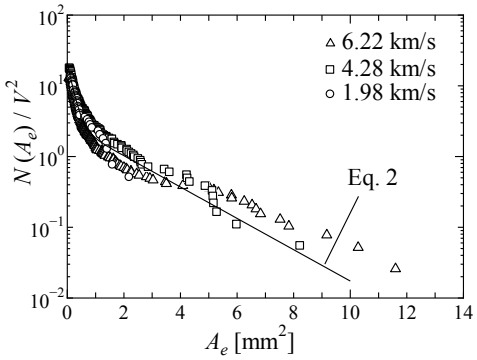

Figure 11. Comparison of experimental results and the bilinear exponential distribution model

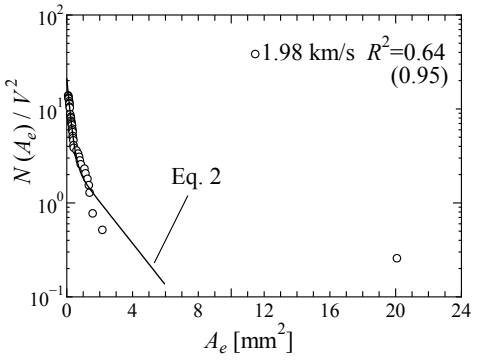

(a) Impact velocity, 1.98 km/s

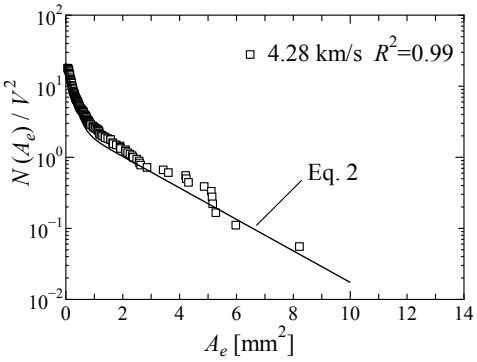

(b) Impact velocity, 4.28 km/s

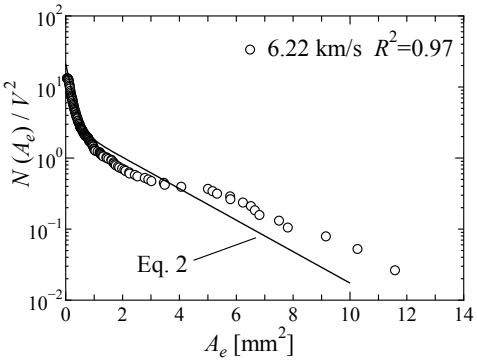

(c) Impact velocity, 6.22 km/s

Figure 12. Coefficient of determination and comparison at each impact velocity

The cumulative number distribution of the projected areas was fitted by a bilinear exponential distribution model.

This work was supported by the Space Plasma Laboratory, ISAS, JAXA as a collaborative program with the hypervelocity impact experiment. This work was supported in part by a Grant-in-Aid for Scientific Research (C), KAKENHI (22560078), from the Japan Society for the Promotion of Science (JSPS).

5 REFERENCES

1. Valerio-Flores, O.L., Murr, L.E., Hernandez, V.S. & Quinodes, S.A. (2004). Observations and simulations of the low velocity-to-hypervelocity impact crater transition for a range of penetrator densities into thick aluminum targets. *J. Mater. Sci.* **39**(20) 6271-6289.
2. Hernandes, V.S., Murr, L.E. & Anchondo, I.A. (2006). Experimental observations and computer simulations for metallic projectile fragmentation and impact crater development in thick metal targets. *Int. J. Impact Eng.* **32**(12) 1981-1999.
3. ISO 11227: 2012, Space systems - Test procedure to evaluate spacecraft material ejecta upon hypervelocity impact (2012).
4. Sugahara, K., Aso, K., Akahoshi, Y., Koura, T. & Narumi, Y. (2009). Intact measurement of fragments in ejecta due to hypervelocity impact. *Proc. 60th Int. Astronautical Cong.* IAC-09-A6.3.06.
5. Siguier, J.M., & Mandeville, J.C. (2007). Test procedures to evaluate space materials ejecta upon hypervelocity impact. *Proc. IMechE.* G **221**, 969-974,
6. Numata, D., Kikuchi, T., Sun, M., Kaiho, K. & Takayama, K. (2007). Experimental study of ejecta composition in impact phenomenon. *Proc. 26th Int. Symp. Shock Waves.* 821-826.
7. Christiansen, E.L., Cytowski, E.D., & Ortega, J. (1993). Highly oblique impacts into thick and thin targets. *Int. J. Impact Eng.* **14**(1-4) 157-168.
8. Nishida, M., Hayashi, K. & Ito, Y. (2012). Effect of impact angles on ejecta and crater shape of aluminum alloy 6061-T6 targets in hypervelocity impacts. *EPJ Web of Conferences.* **26,** 01006.
9. Nishida, M., Kuzuya, K., Hayashi, K. & Hasegawa, S. (2013). Effects of alloy type and heat treatment on ejecta and crater sizes in aluminum alloys subjected to hypervelocity impacts. *Int. J. Impact Eng.* **54**, 161-176.
10. Grady, D. E. & Kipp, M. E. (1985). Geometric statistics and dynamic fragmentation. *J. Appl. Phys.* **58**, 1210-1222.

Leave footer empty – The Conference footer will be added to the first page of each paper.